

PAPER • OPEN ACCESS

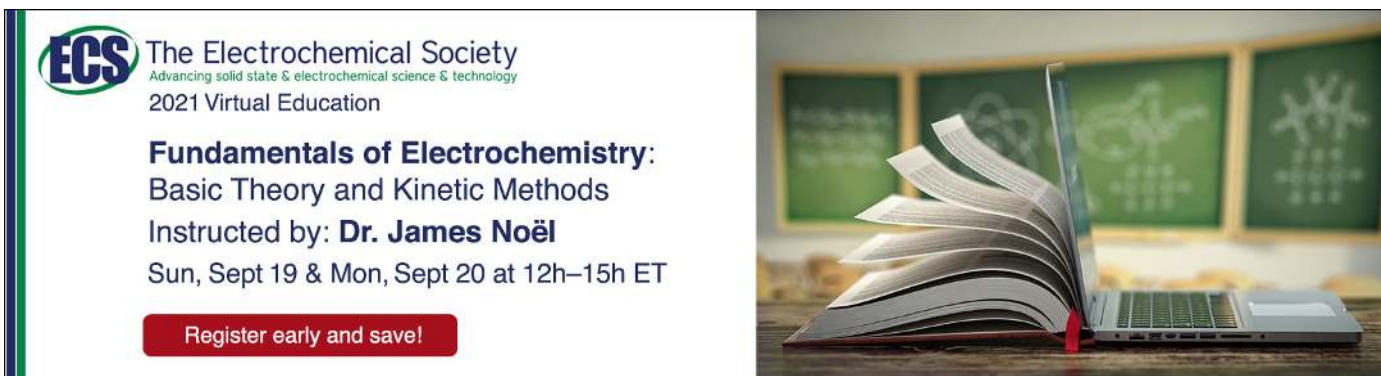
Facile synthesis of CdS Quantum dots for QDSSC with high photo current density

Recent citations

- [Quantum Dot Sensitized Solar Cell: Photoanodes, Counter Electrodes, and Electrolytes](#)
Nguyen Thi Kim Chung *et al*

To cite this article: T Archana *et al* 2020 *Mater. Res. Express* 7 015528

View the [article online](#) for updates and enhancements.



ECS The Electrochemical Society
Advancing solid state & electrochemical science & technology
2021 Virtual Education

Fundamentals of Electrochemistry:
Basic Theory and Kinetic Methods
Instructed by: **Dr. James Noël**
Sun, Sept 19 & Mon, Sept 20 at 12h–15h ET

Register early and save!



PAPER

Facile synthesis of CdS Quantum dots for QDSSC with high photo current density

OPEN ACCESS

RECEIVED

2 November 2019

REVISED

31 December 2019

ACCEPTED FOR PUBLICATION



6 January 2020

PUBLISHED

20 January 2020

Original content from this work may be used under the terms of the [Creative Commons Attribution 3.0 licence](#).

Any further distribution of this work must maintain attribution to the author(s) and the title of the work, journal citation and DOI.

T Archana¹, K Vijayakumar¹, G Subashini², A Nirmala Grace², M Arivanandhan^{1,3}  and R Jayavel¹ ¹ Centre for Nanoscience and Technology, Anna University, Chennai-600025, Tamil Nadu, India² Centre for Nanotechnology Research, Vellore Institute of Technology, Vellore-632014, Tamil Nadu, India³ Author to whom any correspondence should be addressed.E-mail: arivucz@gmail.com

Keywords: quantum dots, stabilizing agent, SILAR, photocurrent density, surface defects

Abstract

Environment-friendly and cost effective green CdS Quantum Dots (QDs) are synthesized using Azadirachta Indica extract as a novel non-toxic stabilizing agent and to excavitate its light harvesting potentiality for QD Sensitized Solar Cells (QDSSCs). The effect of different configuration of green CdS based QDSSCs viz (i) different phase of TiO₂ photoanodes (ii) with and without ZnS passivating layer (iii) with Platinum counter electrodes (CE) and (iv) CuS CE have been investigated. Despite tralatitious SILAR CdS based QDSSC showed better efficiency (1.93%) than green CdS based QDSSC (0.77%), the later unveil higher photocurrent density (10.61 mA) possibly due to effective encapsulation of Azadirachta Indica which suppresses the surface defects in green CdS QDs favoring the transport of photo generated carriers. The work facilitate scope for cost effective and environment-friendly green synthesized CdS QDs that significantly modulated photovoltaic properties of QDs based solar cells in an inviolable condition.

1. Introduction

To meet the increasing energy demands,extensive research have been carried out on photovoltaic technologies over the last several decades. To promote the utilization of photovoltaics as significant energy device, dyes have been replaced with a new type of light absorbing materials namely Quantum Dots. Semiconductor Quantum Dots (QDs) have attracted significant notability as sensitizer material for fabrication of low cost third generation Solar Cells [1–5]. Cd- and Pb- based QDs have been extensively studied for quantum dot-sensitized solar cells (QDSSCs) due to their band gap tunability, quantum confinement, high absorption coefficient, solution processability and near optimal band gap energy [6–9]. QDSSCs are attracting enormous attention and number of relevant research articles is increasing annually. Recently, Luther's group reported highest photoconversion efficiency of QDSSC of 13.43%. Though different strategies have been tried in improving performance and stability of QDs in QDSSCs. There are only limited works reported in controlling the toxicity of QDs that has limited their pervasive use in QDSSCs [10]. The smaller size of nanoparticles can result in the capability to enter to the human body by inhalation, ingestion, skin penetration or injections; thereby, creating the potential to interact with intracellular structures. The toxicity from nanomaterials, specifically because of occupational exposure was studied by European Respiratory Journal (2009), and the health impairments were reported for a period between 5 and 13 months [11]. Better control of nanomaterial toxicity can be done by the safe design of nanoparticles using greener research approach. Consequently, green chemistry-mediated synthesis of QDs is profoundly imperative to reduce its toxicity and extend its applications [12–22].

Manoj *et al* (2019) reported the green synthesis of Cu nanoparticles [17]. Loo *et al* (2012) explained about the synthesis of Ag nanoparticles from *Camellia sinensis* extract [20]. Kavitha *et al* (2018) have green synthesized CdS QDs using tea leaf extract and studied their antimicrobial activity [21]. Recently, copper indium sulphide-based ternary QDs have been fabricated as an alternative to Cd- and Pb-based QDs for QDSSCs; however the former QDs showed lesser efficacy [9]. Moreover, green CdS-based QDSSCs have been rarely investigated.

Further, *Azadirachta Indica* (*A. indica*) is a well-known green source for stabilizing the nanoparticles and used for synthesizing Ag and Pt nanoparticles [15, 16]. However, *A. indica* is not yet used as a stabilizing agent to synthesis CdS QDs. Thus, in the present work, the CdS QDs were synthesized using *A. indica* extract as a stabilizing agent and QDSSCs were fabricated using green CdS QDs. The present work demonstrates the feasibility of using green CdS as a novel approach for improving the performance of QDSSC. QDSSCs were comparatively investigated with different cell combinations and also compared with conventional SILAR CdS-based QDSSCs. For further in-depth study of photoconversion efficiency of green CdS, its sensitizing property analysed at different cell configuration. Different combinations of photoanode phases (anatase and rutile), sensitizers (green CdS and SILAR CdS), counter electrode (Pt and CuS) to increase values of efficiency by improving the light harvesting ability and the electron transfer rate of QDSSCs and by reducing the charge recombination rate at the interfaces [13, 19, 23].

In order to study the phase change induced quantization effect of green CdS, its photoconversion efficiency is studied for both anatase and rutile phase of TiO₂ photoanode [23].

Higher Fermi level of anatase over rutile by 0.1 eV, resulting in a lower oxygen affinity and a higher level of hydroxyl group on TiO₂ surfaces. These hydroxyl groups contribute to the higher photocatalytic activity of anatase. In addition, anatase possesses an indirect bandgap and rutile has a direct band gap. Anatase possesses a wider absorption gap. It is generally proposed that excitation electron mass of the outer shell electrons of anatase is lower than that of rutile, leading to a higher mobility of electrons in anatase. Hence performance of green synthesized CdS is analysed for anatase and rutile TiO₂ coated photoanode.

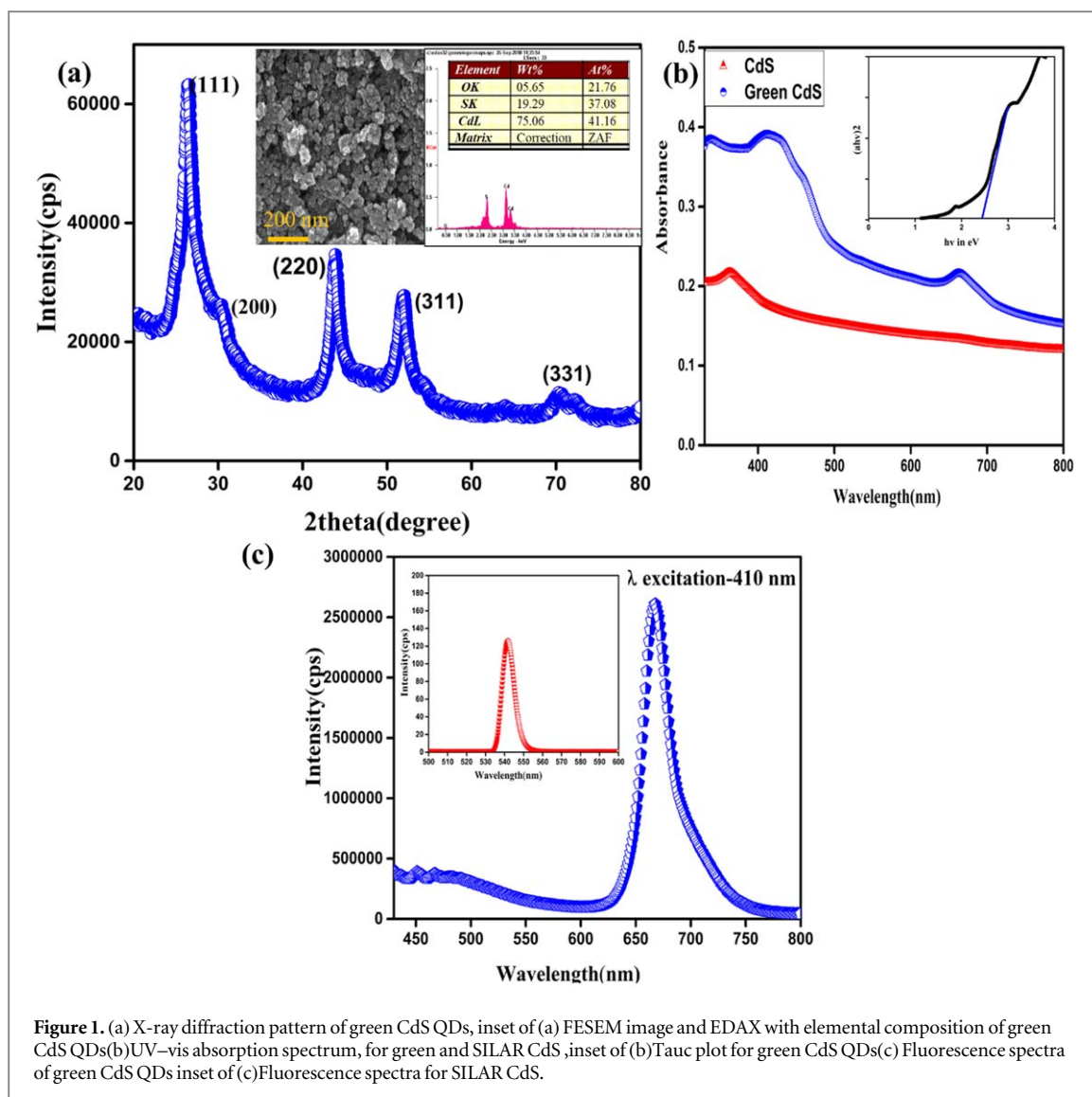
Recent studies on QDSSCs have shown an abate in overall conversion efficiency because of serious electron loss from charge recombination at the electrolyte–electrode or at the electrolyte–counter electrode interfaces. To study on electron losses and to suppress these losses, different approaches such as use of passivating layer, also replacement of Pt counter electrode with CuS have been explored.

2. Experimental

For green synthesis of CdS QDs, *A. indica* plant extract was prepared by following the procedure as reported in the literature [21, 22]. The CdS QDs synthesis was rendered in two stages. In first stage 0.02 M CdCl₂ was added to 50 ml of *A. indica* extract and kept for 3 days in the dark room at ambient temperature. In the second stage, 0.5 ml of 0.025 M Na₂S was added and incubated for 4 days to form CdS nanoparticles. The resultant final solution was yellowish in color with greenish tint. As obtained precipitate was centrifuged at 10000 rpm for 10 min and washed with deionized water for three times [18, 19, 22]. Finally, the obtained product was lyophilized for further characterization studies.

The surface morphology and composition of green CdS were analyzed using Field emission scanning electron microscope with energy-dispersive x-ray analysis (FESEM-FEI Quanta FE G 200). Further, the shape and size of CdS sample were interpreted by high resolution transmission electron microscopy (HRTEM; JEOL TEM 2400). The functional groups of the prepared CdS materials were elucidated by FTIR (Jasco 6600) spectrophotometer. The UV–vis absorption was recorded using Perkin Elmer Optima 5300 DV.

TiO₂ was synthesized by hydrothermal method using TTIP as precursor at 240 °C for 12 h. The obtained TiO₂ was calcined at 500 °C for anatase phase and 700 °C for rutile phase. TiO₂ photoanode was prepared by doctor blade method with active area of 0.25 cm² [23]. Green CdS was loaded on to TiO₂ photoanode by direct absorption method [24]. For comparative analysis, the CdS QDs were loaded on to TiO₂ photoanode using SILAR method too [25]. TiO₂ photoanodes were immersed in solution of 0.4 M CdCl₂ in 1:1 ratio of methanol and water for 45 s followed by rinsing with methanol for 30 s and then immersed in 0.2 M Na₂S solution of 1:1 ratio of methanol and water for 45 s, followed by rinsing with methanol. The deposition temperature was kept at ambient temperature (~32 °C). In this present work, the deposition cycle was chosen as 8 cycles [25–30]. The QDSSC was fabricated by sandwiching QDs loaded photoanode and Pt and CuS counter electrode [31]. The Pt counter electrode was fabricated by using thermal depositing method. In detail, a drop of H₂PtCl₆ solution (5 mM chloroplatinic acid in isopropanol) was dropped onto FTO glass, followed by heating at 400 °C for 15 min. SILAR approach were used to prepare CuS counter electrodes on the FTO substrate. FTO samples were cleaned ultrasonically with acetone, ethanol, and DI water for 10 min each. The cleaned substrates were dried with N₂ gas. The copper sulphide counter electrode was obtained by applying 4 cycles of SILAR using cationic and anionic aqueous solution of 0.5 M Cu(NO₃)₂ and 0.5 M Na₂S. Finally, electrode was dried at 120 °C for 10 min ZnS was coated on the QD loaded photoanodes as a passivating layer (2 cycles) and studied their impact on the performance of QDSSC. The ZnS passivating layer was deposited over the Green CdS and SILAR CdS QDs by 2 cycles of SILAR deposition using aqueous solution containing 0.1 M zinc acetate and 0.1 M sodium sulphide as anionic and cationic source respectively. The polysulphide electrolyte was prepared by 0.5 M sodium sulphide, 0.1 M KCl and 0.2 M sulphur in 7:3 ratio of ethanol and water which was stirred in dark for 5 h [27, 31].



I-V characteristics of the QDSSC were studied by Solar Simulator (1 SUN Oriel Class AAA). Electrochemical impedance spectroscopy (EIS) measurements were recorded by CHI electrochemical workstation (CHI 660C) at frequency ranging from 10 MHz to 100 KHz and impedance spectra were analyzed with EC lab software 1.

3. Result and discussion

Figure 1(a) shows the XRD pattern of green CdS which is well matched with standard JCPDS data (No.10-454) and confirms the cubic structure of CdS. Among the diffraction peaks, (111) peak is having large intensity which shows the preferred orientation of the particles. Broadened diffraction peaks with high full width at half maximum are possibly due to smaller dimension of the particles. Inset of figure 1(a) shows FESEM image and EDAX of green CdS, which confirms the spherical morphology of CdS and the composition of Cd and S along with the presence of weak oxygen peak. Figure 1(b) shows a strong absorption peak centered at 433 nm due to band edge emission of CdS QDs with wide band gap of 2.85 eV (Inset of figure 1(b)). The band gap of prepared QDs is blue shifted as shown in figure 1(b) due to the quantum confinement effect [26–28]. Figure 2(a), b shows the HRTEM images of green CdS particles. The images confirm the spherical morphology of the particles with size of 2–5 nm, which is less than excitonic Bohr radius (~3 nm) of CdS thereby authenticating QD formation thereby the blue shift is observed in figure 1(b). The inset of figure 2(b) shows the HRTEM image of a single QD with clear lattice fringes and the inter planar distance of 0.33 nm [21], which corresponds to preferred orientation of (111) of CdS QDs, as confirmed from XRD pattern (figure 1(a)).

The FTIR spectra of *A. indica* plant extract, green CdS and SILAR CdS are shown in figure 2(c). The IR spectrum of green extract (figure 2(c) (i)) set out double absorption peaks centered at 3435.18 and 3191.18 cm^{-1} is due to primary and secondary amines of plant extract [32, 33]. The peaks at 2949.81 and 2840 cm^{-1} represent

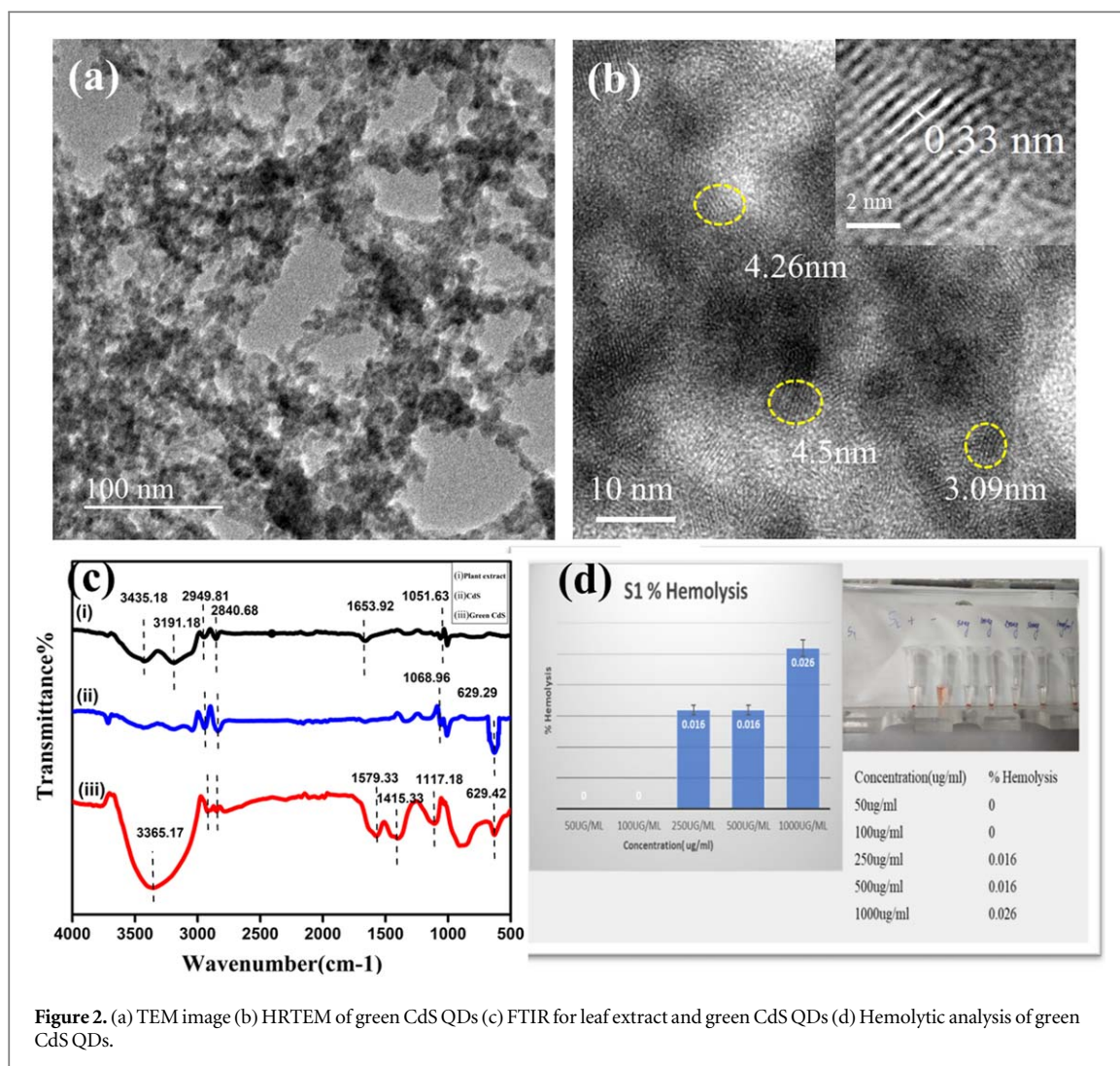


Figure 2. (a) TEM image (b) HRTEM of green CdS QDs (c) FTIR for leaf extract and green CdS QDs (d) Hemolytic analysis of green CdS QDs.

the aliphatic C-H of methanol solvent. The band at 1653.92 cm^{-1} is due to stretching of C=O from ketone groups of *A. indica* and the peak at 1001.9 cm^{-1} is owing to the presence of aliphatic amines. FTIR peaks of green CdS are laid out in figure 2(c) (iii), includes the band at 630.87 cm^{-1} which is the characteristic peak of Cd-S stretching and confirming the formation of CdS QDs. Presence of few organic components can also be observed in FTIR spectrum of green CdS at 1579.33 , 1415.33 and 1117 cm^{-1} due to C-C stretching, O-H bending and C-O stretching, respectively. FTIR spectrum of SILAR CdS (figure 2(c) (ii)) showed peaks corresponding to Cd-S stretching and small intense peaks near 2840 cm^{-1} is by virtue of aliphatic C-H. FTIR spectra uphold the presence of organic molecules probably confounding with the green CdS QDs.

Growth mechanism of green CdS QDs are explained by considering the interaction between the organic molecules of plant extracts and CdS surfaces [33]. Plants extracts have the potential to hyper-accumulate and biologically reduce ions. *A. indica* extract consists of polyphenols, proteins, caffeine, amino acids [33]. Protein binders within the plant extract plays major role in controlling size of CdS, as reducing agent, shape-control modifier and stabilizing agent [34]. At the initial stage, during the addition of cationic source (cadmium chloride) to plant extract, Cd^{2+} ions bind with plant mediated protein due to *in situ* metallic stress from bioactive molecules present in plant extract. On further addition of Na_2S , it facilitates formation of S^{2-} ions and binds to plant mediated Cd^{2+} ions and form CdS QDs. Bioactive components like amines, carboxylic acids, ketones, hydroxyl groups as identified from FTIR spectrum of plant extract (figure 2(c)) plays dominant role in reducing cadmium and then stabilizing them by interacting with Sulphur and forming CdS with controlled sizes and shapes [34]. When organic components or alien ions are attached to growth surface strongly, the available growth sites are occupied, thereby growth process terminates. Presence of small amount of organic residuals with green CdS QDs can be seen from FTIR (figure 2(c)) and EDAX (figure 1(a)) which can act as an organic capping and reducing its toxicity [22]. In addition, Hemolysis assay was performed to evaluate the hemocompatibility of the green CdS QDs and shown in figure 2(d). Green CdS QDs shows the toxicity value of 0.026% which seems to be very low [35]. Further toxicity was analyzed by studying cytotoxic effect of green CdS QDs in

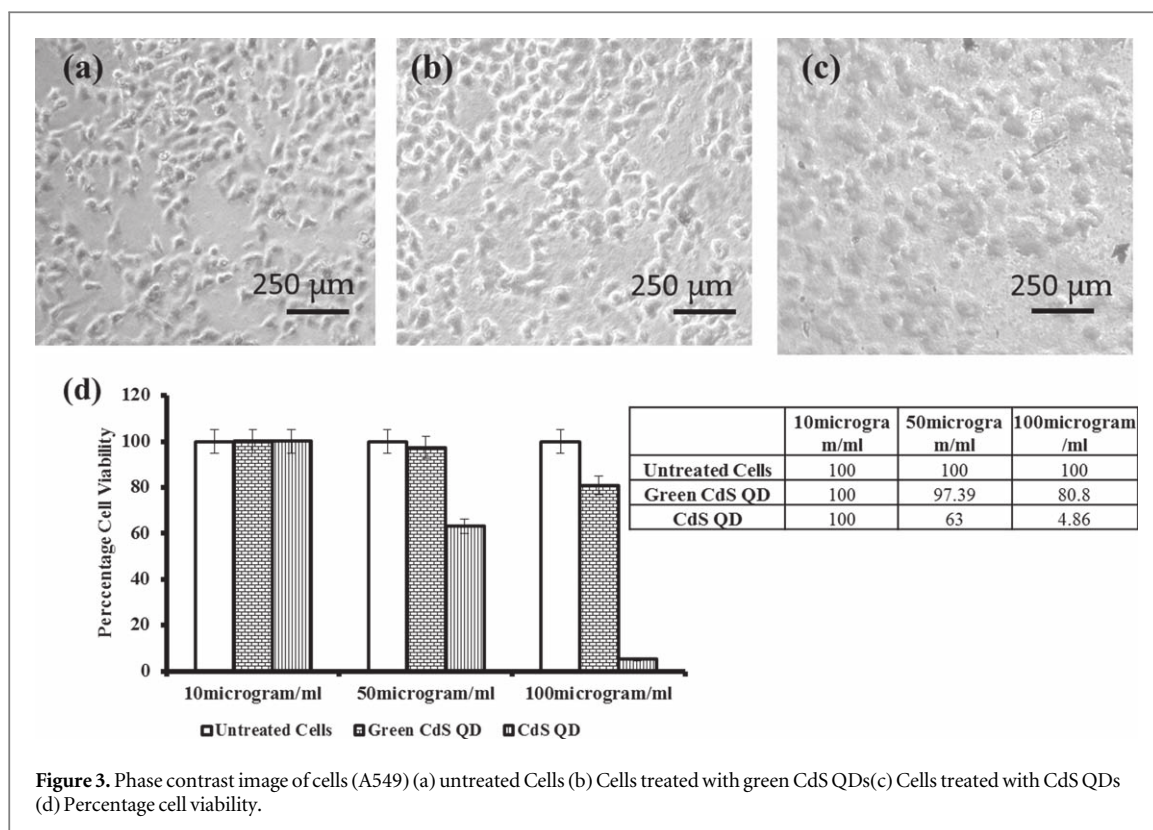


Figure 3. Phase contrast image of cells (A549) (a) untreated Cells (b) Cells treated with green CdS QDs (c) Cells treated with CdS QDs (d) Percentage cell viability.

comparison with CdS QDs [21]. Toxicity is studied on Human lung epithelial cells (A549) and the results are shown in figures 3(a)–(d). Figures 3(a)–(c) gives phase contrast image of cells captured using Lieca DME8 microscope at 40X magnification. The cell morphology at various treatments of QDs is also provided in figures 3(a)–(c). The cell morphology was significantly altered in CdS QDs treated cells compared to Green CdS QDs. The results are shown in figure 3(d). The results indicate that Green CdS QDs does not induce any cytotoxic effect in cell at concentration as high as 100 μg when compared to CdS QDs. The cell viability was only 64% in cell treated with CdS QDs at 50 μg when compared to Green QDs which showed Cell Viability of 97%. The Cell viability was only 4% in CdS QDs at 100 μg concentration when compared to green CdS QDs which showed a viability of 80% at the same concentration. The results indicate that Green CdS QDs does not induce any toxic effect on human cell lines and hence can be considered as nontoxic and environmental friendly in nature.

Figures 4(a) (i) and (ii) showed the XRD patterns of green CdS loaded anatase and rutile TiO_2 photo anodes, respectively. Figures 4(a) (iii) and (iv) are the XRD patterns of SILAR deposited CdS on anatase and rutile TiO_2 photo anodes, respectively. The typical diffraction peaks corresponding to anatase TiO_2 matches with JCPDS card No.21-1272 (figures 4(a) (i) and (iii)) and rutile TiO_2 matches with JCPDS card no: 21-1276 (figures 4(a) (ii) and (iv)). Further, CdS related diffraction peaks are well matched with JCPDS card no: 10-454 which confirms the effective loading of QDs into the photo anodes with different phases. FTO related peaks are also clearly observed in the XRD patterns. UV–vis absorption spectra of green CdS and SILAR deposited CdS loaded TiO_2 with rutile and anatase phases are shown in figure 3(b). The high absorption in visible regime of green CdS loaded photo anode favoring larger absorption window thereby better QDSSC performance [36]. Moreover, green CdS loaded TiO_2 photoanode showed relatively high intensity of absorption compared to SILAR deposited CdS. The presence of auxochromes in organic moieties of green CdS increases the intensity of absorption. Moreover, hypsochromic shift can be seen for green CdS loaded photoanode compared to SILAR CdS owing to confinement effect of Green CdS QDs loaded TiO_2 photoanode. Figures 4(c) and (d) shows the FESEM image and EDAX spectrum of green CdS QDs loaded TiO_2 photo anode, showing effective loading of CdS QDs into the photoanode and the QDs are indicated as yellow color dotted circle in the image (figure 4(c)).

The fabricated QDSSCs were tested with standard (AM1.5) 100 mV solar simulator under 1 sun illumination condition. The obtained cell parameters are shown in table 1. Figures 5(a)–(c) unfold schematic representations of QDSSC with different configurations such as SILAR CdS sensitized QDSSC, green CdS sensitized QDSSC and green CdS based QDSSC with ZnS passivating layer, respectively. Figure 5(d) (i) shows the I–V characteristics of green CdS and SILAR CdS based QDSSCs fabricated using rutile and anatase TiO_2 as photoanodes and platinum as counter electrodes. As can be seen from figure 5(d) (i), the QDSSC with anatase TiO_2 photoanode showed

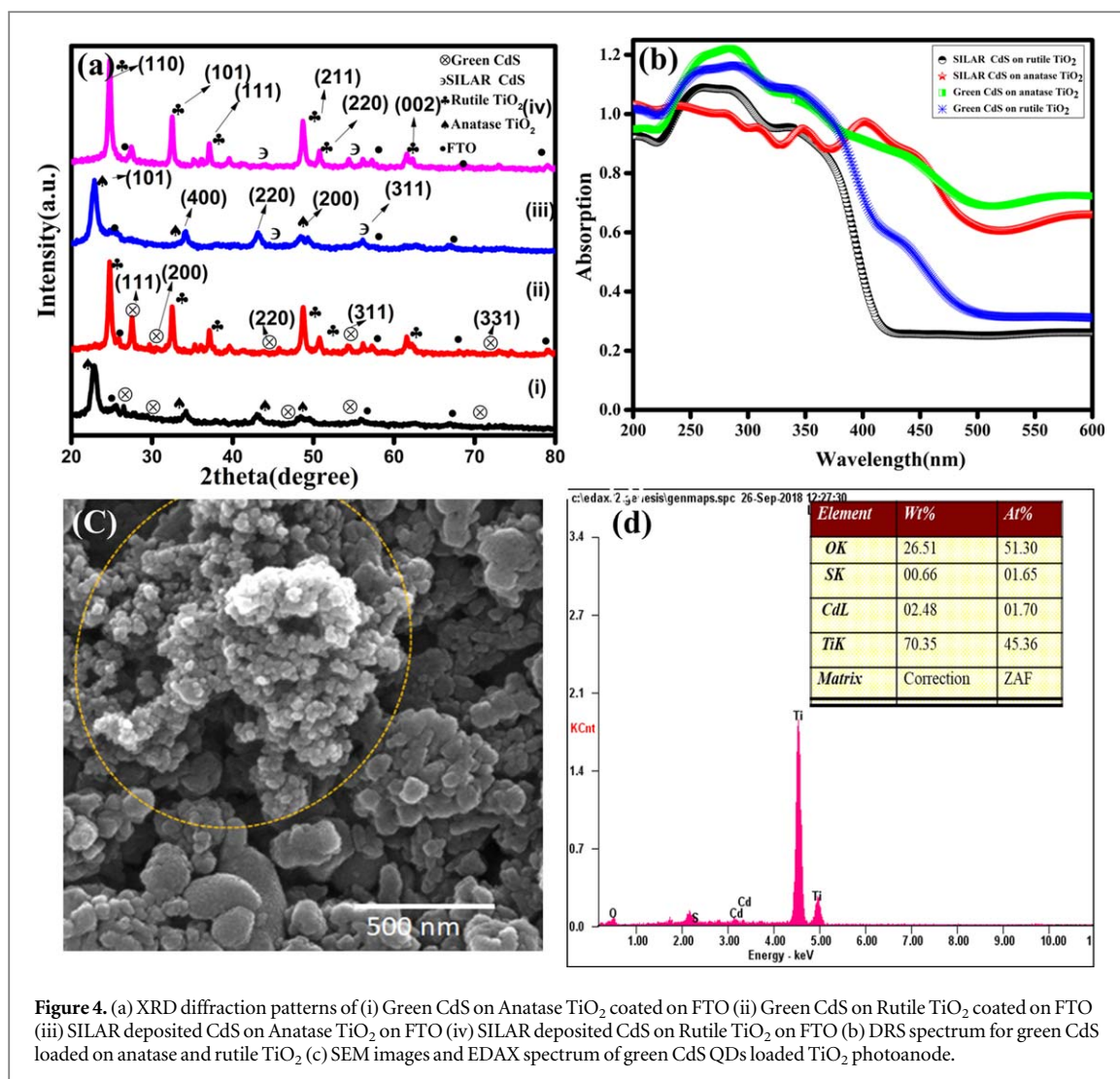


Figure 4. (a) XRD diffraction patterns of (i) Green CdS on Anatase TiO₂ coated on FTO (ii) Green CdS on Rutile TiO₂ coated on FTO (iii) SILAR deposited CdS on Anatase TiO₂ on FTO (iv) SILAR deposited CdS on Rutile TiO₂ on FTO (b) DRS spectrum for green CdS loaded on anatase and rutile TiO₂ (c) SEM images and EDAX spectrum of green CdS QDs loaded TiO₂ photoanode.

Table 1. I–V characteristics of QDSSCs fabricated with different combinations.

Cells	Cell Configurations	Voc (mV)	Jsc mA cm ⁻²	Fill Factor (%)	Efficiency (%)
QDSSC1	Rutile TiO ₂ /Green CdS/Pt	28.7	4.73	23.07	0.02
QDSSC2	Anatase TiO ₂ /Green CdS/Pt	115.1	5.80	28.17	0.19
QDSSC3	Rutile TiO ₂ /SILAR CdS/Pt	343.5	5.90	32.45	0.66
QDSSC4	Anatase TiO ₂ /SILAR CdS/Pt	352.8	9.36	33.98	1.12
QDSSC5	Anatase TiO ₂ /Green CdS/CuS	169.0	10.61	24.80	0.44
QDSSC6	Anatase TiO ₂ /SILAR CdS/CuS	495.9	9.21	47.58	1.36
QDSSC7	Anatase TiO ₂ /Green CdS/ZnS/CuS	258.7	10.56	28.07	0.77
QDSSC8	Anatase TiO ₂ /SILAR CdS/ZnS/CuS	419.3	9.66	47.69	1.93
Ref [30]	CdS (CBD) on TiO ₂	355.0	2.57	18.00	0.17
Ref [31]	CdS (SAM) on std TiO ₂ (p25)	529.0	0.17	59.00	0.05

relatively better performance compared to rutile TiO₂ photoanodes for both kind of green and SILAR CdS QDs. The relatively high performance of anatase TiO₂ photoanodes based QDSSCs are possibly due to the shift in the Fermi level by 0.1 eV compared to rutile phase resulting in a lower oxygen affinity and a higher level of hydroxyl groups on TiO₂ surfaces which favors carrier transport. Anatase possesses an indirect bandgap while rutile has a direct band gap thus minima of the conduction band of anatase is away from the maxima of the valence band, enabling the excited electrons to stabilize at the lower level in the conduction and leading to a longer life (slower charge carrier recombination) and higher mobility than that of rutile with a direct band gap. Also, anatase possesses a wider absorption gap. Excitation electron mass of the outer shell electrons of anatase is lower than that of rutile, leading to a higher mobility of electrons in anatase. Hence improved performance can be observed

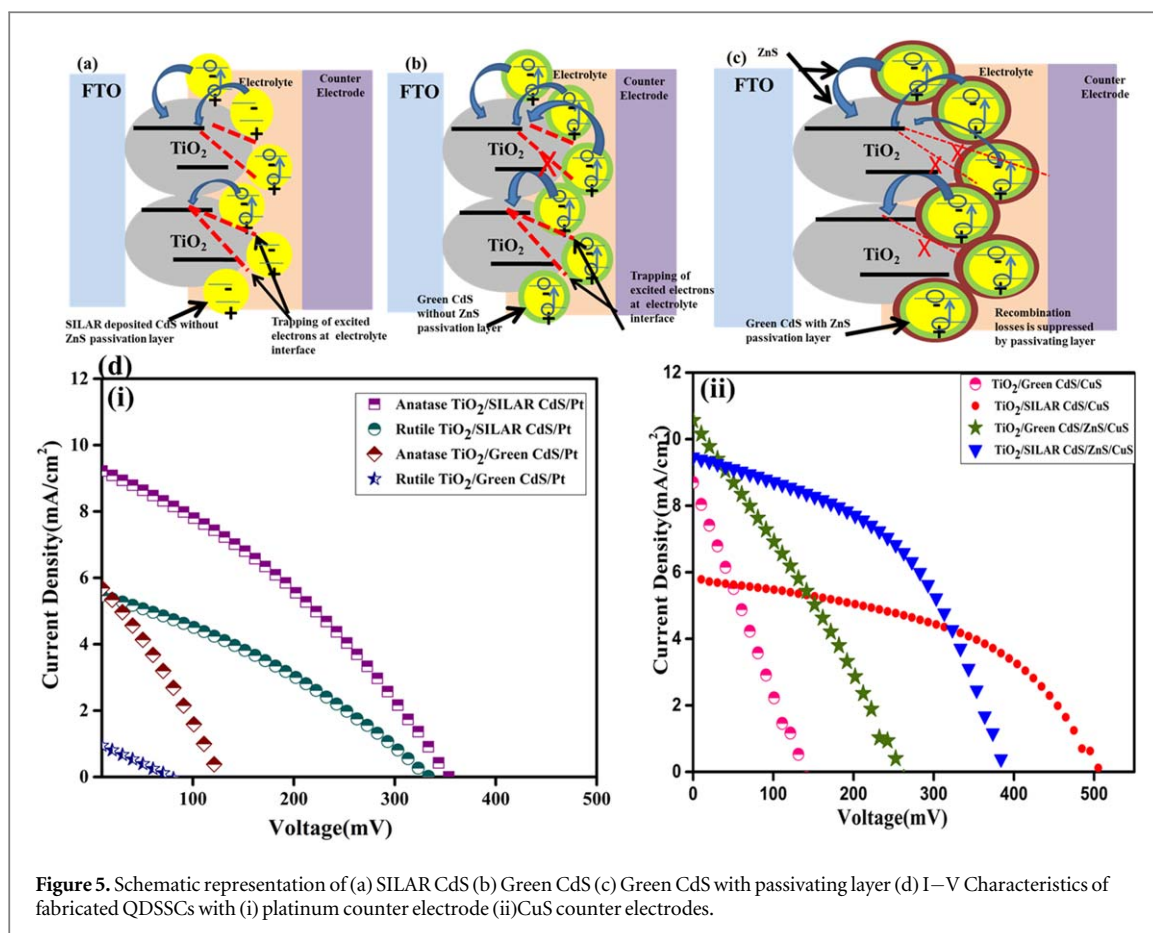


Figure 5. Schematic representation of (a) SILAR CdS (b) Green CdS (c) Green CdS with passivating layer (d) I–V Characteristics of fabricated QDSSCs with (i) platinum counter electrode (ii) CuS counter electrodes.

for anatase phase TiO_2 photoanode with both green synthesized CdS and SILAR deposited CdS [37, 38]. Therefore, the anatase TiO_2 based photoanodes are used for further improving the QDSSC performance by employing the passivating layers and replacing the counter electrodes.

Figure 5(d) (ii) shows the I–V characteristics of green and SILAR CdS loaded anatase TiO_2 based QDSSCs with CuS as counter electrodes. Moreover, the I–V characteristics of the QDSSCs were analysed with and without ZnS passivating layers. As reported passivation layer helps exciton generation in the core to remove defects, such as unsaturated surface atoms on the surface, and to reduce alternative decay pathways and reducing the charge recombination rate at the interfaces. Hence an improved performance can be seen with ZnS layer coating. As can be seen from figure 5(d) (ii), the performance of QDSSC with CuS as counter electrode are relatively high compared to the QDSSC with Pt counter electrode (figure 5(d) (i)). The sulphur from the polysulphide electrolyte may chemisorbs on to the Pt electrode surface, which resulted higher charge resistance at the interface of counter electrode/electrolyte and lowers the performance. Whereas, the ZnS is more compatible with polysulphide electrolyte thereby it shows relatively high performance (figure 5(d) (ii)).

From the I–V curves (figure 5(d) (ii)) it can be inferred that the current density of green CdS based QDSSC is relatively higher (10.61 mA) compared to SILAR CdS based cell (9.2 mA) because of higher visible photon absorption as can be seen from UV–vis spectra (figure 1(b)). The presence of organic moieties with green CdS causes suppression of surface defects and improving flocking of charge carriers. The broadened light absorption from 250 to 520 nm with high intensity favors light harvesting efficiency and presence of retral organic molecules effectively encapsulate the QDs and thereby improved electron hole injection that eventualize improved current density of green CdS based QDSSC. An overall abate in open circuit voltage (V_{oc}) results in lowering of photo conversion efficiency of green CdS based QDSSCs. The decay in V_{oc} is mainly attributed due to recombination losses that deliberately downturn excitonic life time of charge carries. A significant improvement of 65% in V_{oc} is observed for green CdS QDSSC after passivating with ZnS. From the results, it is obvious that the ZnS layer preventing retension of electrolyte towards sensitizer and to TiO_2 photoanode layer that can expedite the recombination of the charge carriers. This phenomenon is schematically shown in figure 5(c). Although more photo-generated carriers are generated in the green CdS, the likelihood of electron-hole recombination is still high. Consequently, the photo conversion efficiency of the green CdS based QDSSCs is lower (0.77%) compared to SILAR deposited CdS (1.93%). Hence much better control of recombination process have to be done for achieving higher conversion efficiency in green CdS sensitized solar cells.

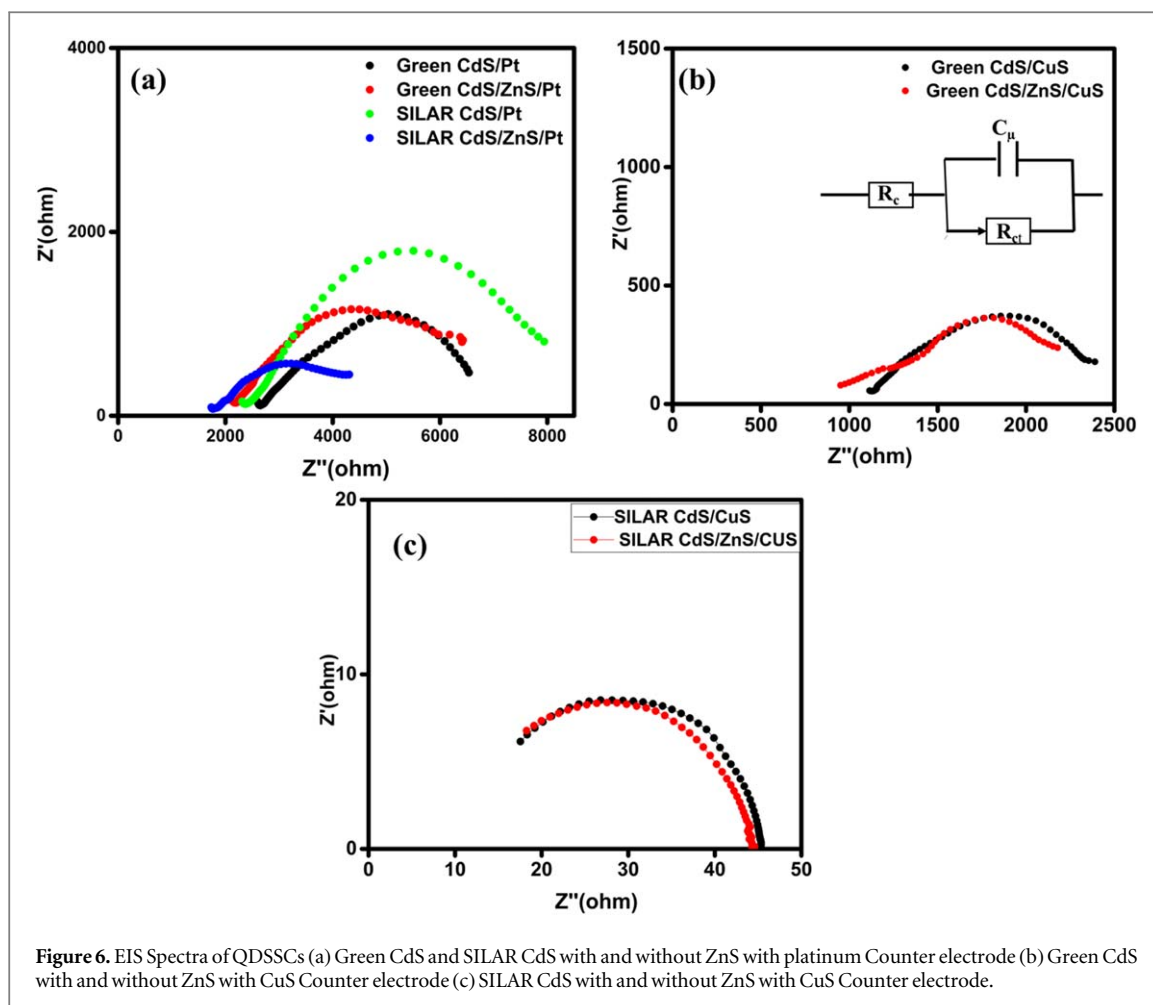


Table 2. EIS characteristics of QDSSCs fabricated with different combinations.

Cell Configurations	R_s (ohm)	R_{ct} (ohm)
TiO ₂ /Green CdS/Pt	2657	331.41
TiO ₂ /Green CdS/ZnS/Pt	2589	231.85
TiO ₂ /SILAR CdS/Pt	2308	301.7
TiO ₂ /SILAR CdS/ZnS/Pt	1735	159.99
TiO ₂ /Green CdS/CuS	976.8	262.9
TiO ₂ /Green/ZnS/CuS	908.5	207.5
TiO ₂ /SILAR CdS/CuS	13.87	15.7
TiO ₂ /SILAR CdS/ZnS/CuS	13.8	11.5

Electrochemical impedance spectroscopy (EIS) analysis is used to evaluate the internal resistance and charge transfer kinetics of QDSSCs. Figures 6(a)–(c) shows the Nyquist plots of green synthesized CdS and SILAR deposited CdS based QDSSCs with platinum and copper sulphide as counter electrodes. The plots were analysed using EC lab software and the obtained parameters from the EIS analysis are summarized in table 2. From EIS data, it is clear that the series resistance values are high for QDSSCs with platinum counter electrodes compared to that with copper sulphide counter electrodes [38–41].

As shown in figure 6, R_s represents the series resistance and R_{ct} represents the charge transfer resistance between counter electrode and electrolyte. The lower R_{ct} value shows higher electrocatalytic activity of CuS based QDSSCs. Relatively higher R_{ct} values of Pt based QDSSC shows the incompatibility of the cell with sulphur based electrolyte which is used in the QDSSC. Therefore, the QDSSCs with CuS as counter electrode showed relatively higher photocurrent compared to cell with Pt counter electrode. Moreover, the QDSSC with ZnS passivating layer showed relatively low charge transfer resistance compared to the cell with no passivating layer. The EIS data revealed that the QDSSC with CuS counter electrode and ZnS passivating layer is an optimum configuration with low R_s and R_{ct} .

4. Conclusion

CdS QDs were synthesized using *A. indica* as a stabilizing agent and its potential ability to enhance the performance of QDSSC were investigated in comparison with conventional SILAR CdS. Green CdS QDs based QDSSCs with ZnS passivating layer showed relatively higher current density 10.61 mA with CuS counter electrode compared to other combinations of cells. The UV-vis absorption spectra revealed the improved optical absorption especially in the visible region for green CdS QDs compared to SILAR CdS QDs based QDSSCs. Surface modification by ZnS passivating layer on green CdS suppress recombination thereby improving the V_{oc} and photo conversion efficiency of green CdS based QDSSC. Further, the experimental results demonstrated that green CdS QDs are favorable as a sensitizer for QDSSCs, as it exhibits the efficiency of 0.76% in a proof-of-concept device. Key research challenges like toxicity of chalcocinides were controlled by effective green synthesis approach resulting QDs with presence of organic moieties without necessarily modifying its electronic property.

Acknowledgments

The author (T A) is grateful to Department of Science & Technology for grant (SR/WOS-A/ET-40/2017) under Women Scientists Scheme A(WOS-A). Authors also acknowledge the financial support of DST-SERB under ECR award (ECR/2015/000575) and EMR (EMR/2016/007550). Author (T A) thank Ms. Sreelakshmi, CLRI for helping us in doing Hemolytic analysis and MTT assay. Thanks to SAIF, IIT Madras for morphological analysis of the samples.

ORCID iDs

M Arivanandhan  <https://orcid.org/0000-0003-4175-2033>

R Jayavel  <https://orcid.org/0000-0001-6270-1484>

References

- [1] Snaith H J, Abate A, Ball J M, Eperon G E, Leijtens T, Noel N K, Stranks S D, Wang J T W, Ojciechowski K W and Zhang W 2014 *J. Phys. Chem. Lett.* **5** 1511
- [2] Yang J, Tang Q, Meng Q, Zhang Z, Li J, He B and Yang P 2017 *J. Mater. Chem. A* **5** 2143
- [3] Kojima A, Teshima K, Shirai Y and Miyasaka T 2009 *J. Am. Chem. Soc.* **131** 6050
- [4] Della Gaspera E, Peng Y, Hou Q, Spiccia L, Bach U, Jasieniak J J and Cheng Y B 2015 *Nano Energy* **13** 249
- [5] Azimi H, Hou Y and Brabec C 2014 *J. Energy & Environmental Science* **7** 1829
- [6] Prabavathy N, Shalini S, Balasundaraprabhu R, Velauthapillai D, Prasanna S and Muthukumarasamy N 2017 *Int. J. Energy Res.* **41** 1372
- [7] Grätzel M 2005 *Inorg. Chem.* **44** 6841
- [8] Kim M R and Ma D 2005 *J. Phys. Chem. Lett.* **6** 85
- [9] McDaniel H, Fuke N, Pietryga J M and Klimov V I 2013 *J. Phys. Chem. Lett.* **43** 355
- [10] Kamat P V 2013 *J. Phys. Chem. Lett.* **46** 908
- [11] Kovacs G, Berghold A, Scheidl S and Olschewski H 2009 *European Respiratory Journal* **34** 888
- [12] Prasad K and Jha A K 2010 *J. Colloid Interface Sci.* **342** 68
- [13] Bai Y Q, Chen J W, Wang L, Li Z, Yang Z, Wen J B, Wang Y F, Jiang J-X and Shi F 2019 *Chem. Phys. Lett.* **723** 170
- [14] Su D, Li P, Ning M, Li G and Shan Y 2019 *Mater. Lett.* **244** 35
- [15] Thirumurugan A, Aswitha P, Kiruthika C, Nagarajan S and Christy A N 2016 *Mater. Lett.* **170** 175
- [16] Velusamy P, Das J, Pachaiappan R, Vaseeharan B and Pandian H 2015 *Ind. Crops Prod.* **66** 103
- [17] Mubayi A, Chatterji S, Rai P M and Watal G 2012 *Adv. Mat. Lett.* **3** 519
- [18] Nadeem M, Tungmunthum D, Hano C, Abbasi B H, Hashmi S S, Ahmad W and Zahir A 2018 *Green Chem. Lett. Rev.* **11** 492
- [19] Felix S, Kollu P, Raghupathy B P, Jeong S K and Grace A N 2014 *J. Chem. Sci.* **126** 25
- [20] Loo Y Y, Chieng B W, Nishibuchi M and Radu S 2012 *Int. J. Nanomed.* **7** 4263
- [21] Shivaji K, Mani S, Ponmurugan P, De Castro C S, Lloyd Davies M, Balasubramanian M G and Pitchaimuthu S 2018 *ACS Applied Nano Materials* **1** 1683
- [22] Pan Z, Mora-Seró I, Shen Q, Zhang H, Li Y, Zhao K, Wang J, Zhong X and Bisquert J 2014 *J. Am. Chem. Soc.* **136** 9203
- [23] Bai Y, Mora-Sero I, De Angelis F, Bisquert J and Wang P 2014 *Chem. Rev.* **114** 10095
- [24] Wang W, Jiang G, Yu J, Wang W, Pan Z, Nakazawa N, Shen Q and Zhong X 2017 *ACS Appl. Mater. Interfaces* **9** 272549
- [25] Ha T T, Lam Q V and Huynh T D 2014 *International Journal of Latest Research in Science and Technology* **2278** 5299 ISSN (Online):2278-5299
- [26] He H, Yang K, Ren S, Liu T and Wang N 2015 *J. Nanomater.* **14**
- [27] Lee Y L and Chang C H 2008 *J. Power Sources* **185** 584
- [28] Zhang Q, Zhang Y, Huang S, Huang X, Luo Y, Meng Q and Li D 2010 *Electrochem. Commun.* **12** 327
- [29] Lee Y L and Lo Y S 2009 *Adv. Funct. Mater.* **19** 604
- [30] Lin S C, Lee Y L, Chang C H, Shen Y J and Yang Y M 2007 *Appl. Phys. Lett.* **90** 143517
- [31] Kim H J, Ko B, Gopi C V, Venkata-Haritha M and Lee Y S 2017 *J. Electroanal. Chem.* **791** 95
- [32] Janakiraman N and Johnson M R 2015 *Journal of Biophysics.* **25** 131
- [33] Pandian S R K, Deepak V, Kalishwaralal K and Gurunathan S 2011 *Enzyme Microb. Technol.* **48** 319

- [34] Jibril D, Mamadou F, Gérard V, Geuye M D C, Oumar S and Luc R J 2015 *Chem. Sci.* **5** 52
- [35] Dobrovolskaia M A, Clogston J D, Neun B W, Hall J B, Patri A K and McNeil S E 2008 *Nano Lett.* **8** 2180
- [36] Gao X X, Ge Q Q, Xue D J, Ding J, Ma J Y, Chen Y X, Zhang B, Feng Y, Wan L J and Hu J S 2016 *Nanoscale* **8** 16881
- [37] Kumar A, Li K T, Madaria A R and Zhou C 2011 *Nano Res.* **4** 1181
- [38] Liu D, Liu J, Liu S, Wang C, Ge Z, Hao X, Du N and Xiao H 2019 *J. Mater. Sci.* **54** 4884
- [39] Kumar K A, Pandurangan A, Arumugam S and Sathiskumar M 2019 *Sci. Rep.* **9** 1228
- [40] González-Pedro V, Xu X, Mora-Sero I and Bisquert J 2010 *ACS Nano* **4** 5783
- [41] Yu Z, Zhang Q, Qin D, Luo Y, Li D, Shen Q, Toyoda T and Meng Q 2010 *ElectrochemistryCommunications* **12** 1776